Int. J. Electron. Commun. (AEÜ) 112 (2019) 152936

Contents lists available at ScienceDirect

International Journal of Electronics and Communications (AEÜ)

journal homepage: www.elsevier.com/locate/aeue

Regular paper

Magnitude-only modeling for sigma-delta modulator characterization

Konstantinos Touloupas *, Paul Peter Sotiriadis

School of Electrical and Computer Engineering, National Technical University of Athens, Heroon Polytechniou 9, 15780 Zografou, Greece

ARTICLE INFO

Article history:
Received 19 July 2019
Accepted 29 September 2019

Keywords:
Sigma-delta
Noise transfer function
Modeling
Vector fitting

ABSTRACT

Sigma delta modulators importance is unambiguous in many applications. Since they are inherently non-linear systems, they are often approximately linearized to allow for the derivation of their theoretical Noise-Transfer-Function (NTF). SDM NTF is used for both analyzing and synthesizing them. Although linearization is the standard approach for its derivation, there do exist SDM architectures to which it cannot be applied. The aim of this paper is twofold: To provide a general framework for deriving the NTF for all SDM architectures, and, to use it to evaluate the accuracy of the standard theoretical NTF approximation for those SDM architectures accepting linearization. To this end, we introduce a new magnitude-only transfer-function modeling framework for SDM architectures, which is based on output noise spectrum and produces a stable LTI NTF approximation model. This framework is based on a phase reconstruction and a rational transfer-function fitting step, using the Vector Fitting algorithm. To show its applicability, we used it to derive NTF models for SDMs at system level and at RTL. Finally, the generality of our approach is demonstrated by deriving experimental NTF for a class of SDMs without standard linearized models.

1. Introduction

Advancement in digital CMOS IC technology has resulted in powerful digital circuits dominating modern electronics systems and even replacing traditional analog operations. The interface to the physical world, however, requires the use of digital-to-analog (DAC) and analog-to-digital data converters (ADC). When high resolution data conversion is needed, Sigma-Delta modulators (SDM) are an excellent choice in many cases [1–4]. Many other systems also rely on SDMs, including fractional-N PLLs [5–8], all-digital transmitters [9–11], class-D power amplifiers [12–14], signal converters [15–17], etc.

SDM is a non-linear feedback loop with a filter and a quantizer as shown in Fig. 1. The purpose of the SDM is to pass the input signal to its output, representing it with the resolution of the quatizer, which can be 1 or more bits, and with the minimum possible quality loss [18]. It typically samples the input signal at a rate much higher than the Nyquist rate corresponding to the signal's bandwidth and shifts the power of the quantization error(noise) outside of the useful frequency band. The ratio between the SDM sampling rate and the Nyquist rate is known as the oversampling ratio (OSR).

It is essential to have an analytical system model of the SDM and use it to analyse or design the SDM's input–output behaviour. For this purpose, it is a common practice to replace the quantizer (a stongly nonlinear element) with a linear 'approximately-equivalent' block formed of a static gain k and an additive noise source, as in Fig. 2. Furthermore, in most cases it is assumed that $k = 1$ and the additive noise is white [18].

This approximate linearization leads to the equivalent two-input single-output system,

$$Y(z) = STF(z)X(z) + NTF(z)W(z), \tag{1}$$

where $X(z)$ and $W(z)$ are the z-Domain transforms of the input signal and the additive white noise. The Signal Transfer Function (STF) and Noise Transfer Function (NTF) are given by

$$STF(z) = \frac{L(z)}{1 + L(z)} \tag{2}$$

and

$$NTF(z) = \frac{1}{1 + L(z)}. \tag{3}$$

Based on (1) the output is composed of the input weighted by $STF(z)$ and the quantization noise component $NTF(z)W(z)$, both of which are functions of the loop filter L. Typically, L is selected so that STF is very close to unity and NTF is very close to zero within the useful signal bandwidth, and, the loop is stable [18,19].

Apart from this approach, other techniques have been proposed for the analysis and modeling of SDM operation inluding quasi-linear analysis [20,21], state-space models with nonlinear dynamics [22], limit cycle analysis [23], parallel decomposition [24], etc.

* Corresponding authors.
E-mail address: ktouloupas@mail.ntua.gr (K. Touloupas).

https://doi.org/10.1016/j.aeue.2019.152936
1434-8411/

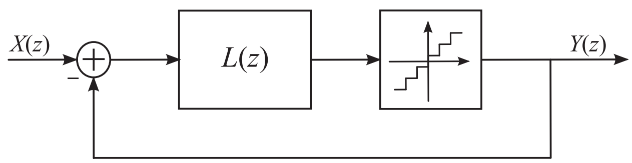

Fig. 1. System diagram of an SDM.

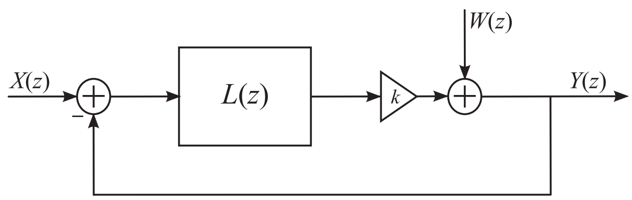

Fig. 2. Linear SDM model where the quantizer is replaced by a static gain k and an additive error(noise) signal w.

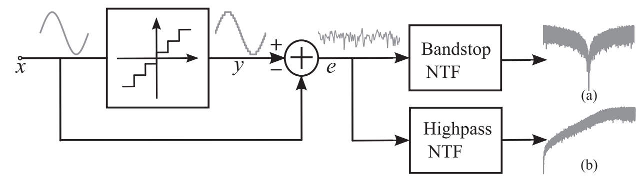

Fig. 3. The noise shaping procedure of an SDM, illustrated for a) a bandstop and b) a highpass NTF. The difference between input and the output of the quantizer is a white noise signal, which is shaped by the NTF.

All these approaches are also approximate and their accuracy depends on the parameters of the particular SDM studied.

Since the definition and derivation of NTF is necessary, an alternative approach, using only input–output data, was proposed in [25,26]. In this setting, SDM behaviour is modeled as a black box by an autoregressive moving average model with exogenous inputs (ARMAX). The SDM is excited with an odd random-phase multisine and the resulting frequency domain output samples are fitted to the model [25–27].

Inspired by the above methodology in [25], this work introduces a new approach in defining and deriving the NTF of SDM, based on a magnitude-only modeling technique. Instead of using ARMAX, the introduced approach models NTF directly as a stable rational transfer function. It assumes an internal white noise source of unit power, as noise input, while the SDM is excited by a single sinusoidal signal. First the power spectral density of the output noise is calculated and filtered to reconstruct the phase. Then, the resulting complex-valued spectral samples are used to determine the magnitude response of the SDM NTF at a predetermined set of frequencies. Finally, these frequency samples are used in the popular Vector Fitting algorithm [28], which delivers a rational transfer function fitting the samples in magnitude.

The contributions of this work are 1) a framework for magnitude-only modeling of transfer functions using the Vector Fitting algorithm and the phase reconstruction procedure, 2) application of this framework to deriving the NTF of SDMs, and 3) comparison of the derived NTF with the theoretical linearized models and verification of the last ones.

The paper is organized as follows: Section 2 describes properties of conventional SDMs that are used in the proposed methodology. In Section 3, the proposed approach for magnitude-only modeling is presented and the reader is introduced to the Vector Fitting algorithm. Section 4 provides system-level and RTL simulations using both conventional SDMs and SDMs not accepting the simple linearization. Section 5 concludes the discussion.

2. SDM Properties

In order to generate an output signal with low quantization noise floor within the frequency range of interest, Sigma-Delta Modulation relies on two fundamental properties, oversampling of the input signal and quantization error spectrum shaping. Oversampling results in output noise power spectral density reversely proportional to the OSR, i.e.,

$$S_W = \frac{\Delta^2}{12 * \text{bandwidth} * OSR}, \tag{4}$$

under the assumption that the quantization error is approximately uniformly distributed white noise for realistic input signals [18]. Here, Δ is the step of the quantizer.

In-band output noise is further reduced by shaping the output quantization noise power, via NTF, outside the frequency band of interest. To this end, the magnitude of the NTF is small within the frequency band of interest (in-band) and equivalently, the magnitude of the loop filter, $L(z)$ is large because of (2), also implying that the STF is close to unity. This error shaping procedure is illustrated intuitively in Fig. 3[29].

SDM synthesis is equivalent to the selection of an NTF that maximizes the signal-to-quantization-noise ratio (SQNR) [18] in the frequency band of interest, while ensuring stability and reasonable hardware complexity. NTF design is typically done by appropriately placing its zeros and poles, separately. Note that the designer should also consider the loop filter stability and the need for the NTF to be a causal filter, in order for the SDM to be realizable [29].

Besides the conventional SDM in Fig. 1, several alternative architectures have been proposed and used in state-of-the-art systems, providing trade-offs between hardware complexity and noise suppression. Of great interest are the MASH SDMs, providing low hardware implementation complexity [30,31], and the recently introduced Multi-Step Look-Ahead SDMs, providing higher stability range and better noise suppression with a small hardware overhead [32].

The aforementioned properties are used in the following section to establish our modeling methodology.

3. Magnitude-only modeling of SDM NTF

Designing and verifying SDMs is a critical and usually cumbersome process when the requirements are stringent, typically in many signal generation and processing systems like advanced frequency synthesizers, data converters etc [33]. Having a model of the SDM transfer functions is necessary to estimate the total behaviour of the overall system to which the SDM is a part. However, the definition and derivation of the NTF especially is not trivial, as NTF is a conceptual filter which cannot be excited directly or indirectly.

The proposed approach defines and derives the NTF of the SDM based on frequency-domain fitting and leveraging the whiteness property of the SDM quantization noise, while avoiding cumbersome time-domain system identification for SDMs with binary outputs [34].

The resulting model has the same output noise PSD as the SDM and it is derived entirely from frequency domain magnitude data, since the phase of the NTF input signal is unavailable. Furthermore, unlike prior work on magnitude-only macromodeling [35,36], which require the solution of constrained minimization problems and doubling of the model order complexity, the proposed framework solves repeatedly linear systems. This results in both higher computational efficiency and convergence rate.

Assumption: *The quantization error is white noise with unit power spectral density, i.e.* $S_W(e^{j\omega}) = 1$.

The assumption along with the definition of NTF imply that the PSD of the output noise, $S_n(e^{j\omega})$, is such that

$$|NTF(e^{j\omega})| = \sqrt{S_n(e^{j\omega})}. \tag{5}$$

Note that the assumption of $S_W(e^{j\omega}) = 1$ is made only to simplify the mathematical expressions and notation. To account for any values of Δ and OSR, and so for $S_W(e^{j\omega}) \neq 1$, one can follow the steps of the proposed approach and divide the derived model function by $\sqrt{S_W(e^{j\omega})}$.

The function $|NTF(e^{j\omega})|$ of $\omega \in [0, \pi]$ is derived in numerical form via simulation of the SDM and the data are used in the phase reconstruction stage of our approach. Following, a frequency domain model is derived using the Vector Fitting algorithm.

3.1. Phase reconstruction

Phase reconstruction is the first stage of the proposed approach. It supplements the available magnitude-only data from (5) with artificial phase following the *minimum phase* and *all-pass deconvolution* method [37].

If NTF is a minimum-phase rational transfer function, its phase is uniquely defined by its magnitude and it coincides with the generated phase data. If instead NTF is of non-minimum phase, the proposed approach yields data that correspond to a minimum-phase function with the same magnitude.

Let us consider a stable sequence $p[n]$ and its z-transform $P(z)$. If $ln(P(z))$ has a power series expansion converging within the unit circle, then the complex cepstrum of $p[n]$ exists and can be expressed as in [37].

$$p[n] = p_{min}[n] * p_{ap}[n]. \tag{6}$$

The Fourier transform of (6) implies that $P(e^{j\omega})$ is the product of a minimum phase and all-pass component, i.e.:

$$P(e^{j\omega}) = P_{min}(e^{j\omega}) \cdot P_{ap}(e^{j\omega}). \tag{7}$$

Consider $NTF(e^{j\omega})$ in the place of $P(e^{j\omega})$. Since $|NTF_{ap}(e^{j\omega})| = 1$, the minimum phase component, $NTF_{min}(e^{j\omega})$ has the same magnitude with $NTF(e^{j\omega})$. Using the available magnitude of the $NTF(e^{j\omega})$, we determine the minimum phase component of the NTF, using the procedure illustrated in Fig. 4.

Summarizing the procedure for the phase reconstruction, first $|NTF(e^{j\omega})|$ is estimated at a set of frequencies $\omega_k \in [0, \pi], k = 0, 1, \ldots, N_s - 1$, using simulation or measurements and (5); then, the values $NTF_{min}(e^{j\omega_k}), k = 0, 1, \ldots, N_s - 1$ are derived as in Fig. 4 [37]. Sequence $NTF_{min}(e^{j\omega_k})$ has the right amplitude and a reconstructed phase.

3.2. z-Domain vector fitting for SDM

The N_s frequency response samples $H(e^{j\omega_k}), k = 0, \ldots, N_s - 1$, derived using the procedure in the previous subsection, are fed to the z-Domain version of the Vector Fitting algorithm [38], which is denoted by VF for simplicity.

VF fits a pole-residue model (8) to the samples in the least squares sense, i.e.,

$$NTF_{min}(z) \approx \sum_{n=1}^{N} \frac{R_n}{z - p_n} + R_0. \tag{8}$$

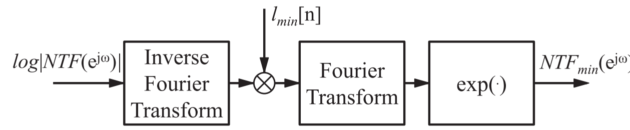

Fig. 4. Derivation of the equivalent $NTF_{min}(e^{j\omega})$ with reconstructed phase. $l_{min}[n] = 2u[n] - \delta[n]$.

Residues R_n and poles p_n may be real or complex conjugate pairs, while R_0 is real. Model order N is selected a priori. In our case, One option is to select N equal to the order of the SDM loop filter $L(z)$.

The algorithm is comprised of two steps, the *pole relocation* and the *residue identification*.

In the pole relocation step, the poles $p_n, n = 1, 2, \ldots, N$ are derived. Since the direct least squares solution of (8) is a nonlinear problem, an iterative procedure is used instead, which is a special case of the Steiglitz-McBride method [39]. Here, the model in the right hand side of (8) is expressed as $N(z)/D(z)$ with its numerator and denominator having the following form:

$$N(z) = \sum_{n=1}^{N} \frac{\bar{c}_n}{z - a_n} + \bar{c}_0, \quad D(z) = \sum_{n=1}^{N} \frac{\bar{d}_n}{z - a_n} + 1. \tag{9}$$

Quantities $\bar{c}_n, \bar{d}_n, a_n, n = 1, \ldots, N$ are real or come in complex conjugate pairs and $\bar{c}_0$ is real. Note that $N(z), D(z)$ share the same poles and therefore the poles of the model in (8) are in fact the zeros of $D(z)$.

Multiplication of the error $NTF_{min}(z) - N(z)/D(z)$ with $D(z)$ and substitution from (9) yields the minimization problem [1]:

$$\left[\sum_{n=1}^{N} \frac{\bar{d}_n}{z - a_n} + 1\right] NTF_{min}(z) - \left[\sum_{n=1}^{N} \frac{\bar{c}_n}{z - a_n} + \bar{c}_0\right] \approx 0. \tag{10}$$

By selecting an initial set of parameters a_n, (10) becomes linear in $\bar{d}_n, \bar{c}_n$ and $\bar{c}_0$ and it is solved using least squares. Parameters $\bar{d}_n$ and a_n are used to compute the zeros of $D(z)$ which are then used as the updated values for a_n.

This results in a new minimization problem (10). Parameters a_n are called the *relocated poles*. The above procedure is repeated for a predefined number of iterations with a_n typically converging to certain values [40]. The poles p_n of the model are selected as the last set of relocated poles a_n.

The resulting model is required to be stable, so if an iteration results in an unstable relocated pole a_n, i.e. $|a_n| > 1$, this pole is replaced by $1/a_n^*$ [41].

In the residue identification step, parameters $R_n, n = 0, \ldots, N$ of (8) are derived. Since the poles of the model are found in the pole relocation step, (8) can be solved for the residues in the least-squares sense. For the reader's convenience, an overview of the algebraic details of the algorithm is presented in the Appendix.

3.3. Numerical considerations

The problems in (8) and (10) are solved using linear least squares. The non-smooth spectral data, exhibiting large amplitude variations, used as input samples of the VF algorithm, make the least squares systems (8) and (10) prone to errors. To combat the above obstacle, our approach includes the following pre-processing steps:

1) Filtering of the spectral data: The spectral data are not smooth and neighbouring samples may vary several dBs in magnitude. To reduce the effect of these variations, the samples are filtered using

[1] The number of samples is typically much larger than the model order N.

a zero phase lowpass filter. In addition, a non-uniform selection of the sampling frequencies with emphasis on the in-band (low-noise) frequencies can help further deriving a more accurate model.

2) Frequency Weighting: Solving the problem in (10) using regular least squares implies a uniform treatment of all frequencies independently of the actual power spectral density function of the noise. This results in good approximation in frequencies with strong noise but poor approximation in low-noise bands, typically in the in-band of the SDM. To address this issue, frequency weighting is used. This is done by multiplying both sides of (10) and (8) with vector $\boldsymbol{w}$,

$$\boldsymbol{w} = diag\{w_1, \dots, w_{N_s}\}, \tag{11}$$

where every weighting coefficient w_i corresponds to a single frequency sample and is set equal to the reciprocal of the sample's magnitude.

4. Simulations and results

In this section the proposed modeling approach is illustrated using a number of examples. Since it is applicable to all SDM architectures, we demonstrate its efficacy on both conventional and MSLA SDMS at system level and at RTL.

In all examples, a sinusoidal input within the useful bandwidth of the SDMs is applied and the output noise spectrum is obtained by subtracting the input signal from the SDM output [2]. The choice of sinusoidal excitation signals for SDM NTF excitation is standard in the literature [18,42]. The derived results are compared with the theoretical estimates based on linearization of the SDMs. The experiments are executed on a quad-core i7 machine at 2.7 GHz with 8-GB RAM, running MATLAB 2017b.

4.1. System-level lowpass SDM

Consider a single-bit output, lowpass SDM, with third order NTF and OSR of 128. The modulator is implemented at system level using the Delta-Sigma Toolbox [43]. The NTF is designed using optimal placement of zeros. A sinusoidal signal of 0.1 amplitude is used for excitation. We choose the frequency (divided by the sampling frequency) of the sinwave, to be 0.0006 rad/s. The simulation provided 2^{17} SDM output data samples.

Order $N = 3$ is chosen for the VF model and the maximum number of iterations is set to 30. The spectral data were filtered and frequency weighting was applied, as described in the previous section.

The frequency response of our NTF model is depicted in Fig. 5, along with the available data and the theoretical NTF. There is very good agreement between our model and the theoretical NTF, in almost all frequencies.

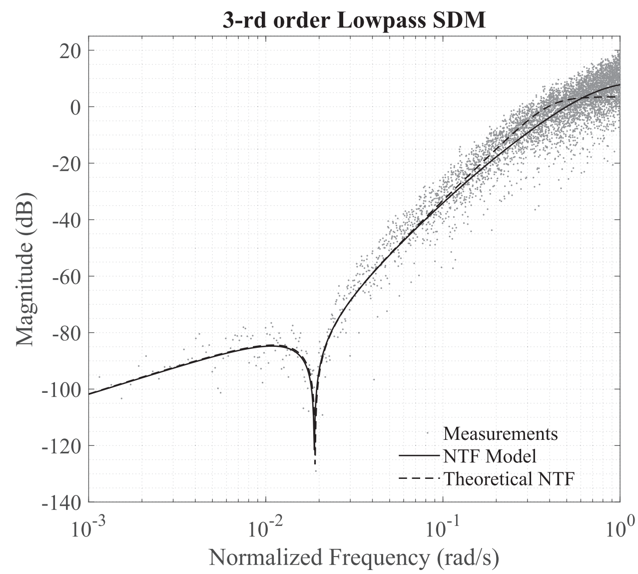

Fig. 5. Comparison of the derived NTF with the theoretical NTF based on the linearized SDM and with the measurements. Measurements appear decimated for demonstration purposes.

4.2. System-level bandpass SDM

Here, we apply the proposed approach to a bandpass SDM with OSR of 128, 4-th order NTF and with normalized central frequency of about 0.63 rad/s. The modulator is implemented at system level using the Delta-Sigma Toolbox and it is excited by a sinusoidal signal of amplitude 0.1 inside the bandwidth of the filter. The NTF is designed with optimal zero placement. SDM simulation produces 2^{17} output data samples.

Similarly to the lowpass SDM case, the spectral data are filtered and frequency weighting is applied as well, emphasizing the in-band noise shaping dynamics. Order of $N = 4$ is selected for the VF derived NTF model.

Fig. 6 illustrates the accuracy of the derived NTF model with respect to the theoretical NTF and the measured data. It is shown that our approach generalizes well to the bandpass class of SDMs. The model is in very good agreement with the theoretical transfer function.

4.3. RTL implementation of bandpass MSLA SDM

An advantage of the proposed approach is its direct applicability to all SDM architectures due to its black-box nature. In this subsection the test case is a hardware implementation of a bandpass MSLA SDM.

Note that there is no established analytical model for the MSLA SDM NTF [32]. Therefore, the proposed approach provides a way to define and derive the NTF. To demonstrate the application, we choose a single-bit-output MSLA SDM with $k = 3$ look-ahead steps, 8-th order bandpass filters and OSR equal to 128, [32].

A general form of MSLA SDM architecture is shown in Fig. 7. In contrast to conventional SDMs, the MSLA has multiple loop filters and a multi-input quantizer [32]. In our case of $k = 3$ look-ahead steps, there are 4 loop filters and a 4-input single-bit output quantizer. Each loop filter consists of 3 FIR (finite impulse response) filters and a single IIR (infinite impulse response) filter. The 4-input single-bit output quantizer is a static function and it is implemented as a LUT. A detailed theoretical analysis, derivation and parametrization of this MSLA SDM architecture can be found in [44].

The hardware implementation of the loop filters was done using high-level design techniques that generate HDL code. The LUT entries that implement the quantizer are pre-calculated using MATLAB and partitioned in 38-sub LUTs to reduce the required address bits for each sub-LUT. The LUT entries complexity depends on the number of bits used for the representation of the quantizer's input. By following the optimization steps described in [44], we were able to use 6-bit logic for the quantizer input and 32-bit fixed-point arithmetic for the FIR and IIR filters of each loop filter.

[2] STF is considered unity with the bandwidth of the SDM.

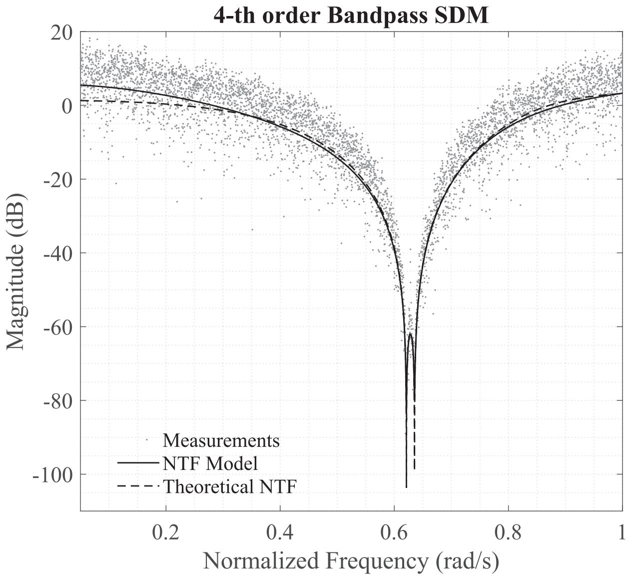

Fig. 6. Comparison of the derived NTF with the theoretical NTF based on the linearized SDM and with the measurements. Measurements appear decimated for demonstration purposes.

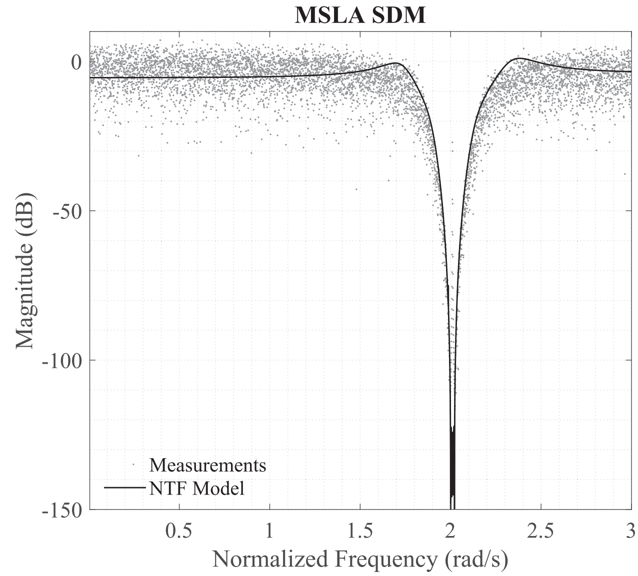

Fig. 8. Comparison of our model accuracy with the collected spectrum data. Please note that the output noise spectrum data are decimated before plotting, for demonstration purposes.

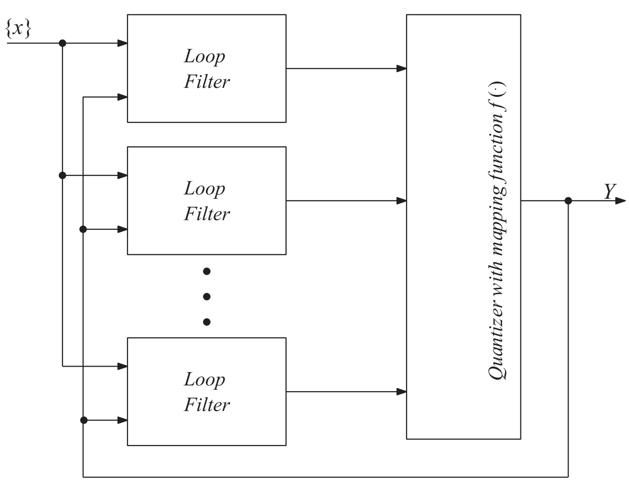

Fig. 7. MSLA SDM effiecient-form system diagram.

Table 1
MSLA SDM hardware resources.

Resource	MSLA SDM
Max. output rate [Msamples/s]	13.3
Slice LUTs [Used Util.]	23,342/11.45%
Slice Registers [Used/Util.]	1,665/0.41%
F7 Muxes [Used/Util.]	2,331/2.29%
F8 Muxes [Used/Util.]	650/1.28%
DSP Blocks [Used/Util.]	205/24.40%

The MSLA SDM was implemented for a Xilinx Kintex-7 KC705 Evaluation Kit target device. Table 1 summarizes the hardware resources used for the FPGA implementation.

The output data of the MSLA SDM were collected by digital simulation, after placement and routing. A sinusoidal signal generated by a 24-bit direct digital synthesizer (DDS) with amplitude 0.25 and normalized frequency $0.628 \times \pi$ rad/s is used as stimulus. Four million output samples were collected and used for the NTF modeling of the SDM. The model order in the VF algorithm was set to $N = 12$ and spectrum data filtering and weighting was applied.

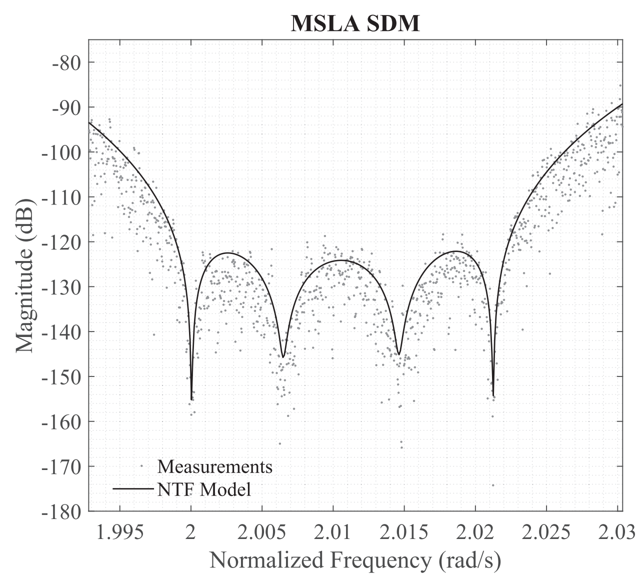

Fig. 9. Comparison of our model accuracy with the collected spectrum data. Zoom-in of the MSLA SDM spectral data.

The magnitude response of the derived NTF model is shown in Fig. 8 in comparison to the square root of the measured output noise spectrum of the MSLA SDM. For better illustration, Fig. 9 demonstrates the in-band response of the derived NTF model. It appears that the model captures the output noise shaping of the modulator in the entire frequency band with accuracy.

5. Conclusion

An approach for the estimation of the SDM NTF which is applicable to all SDM architectures and demonstrates good accuracy was presented. By definition, the SDM NTF is a conceptual filter and its input is not available. Thus, we introduced a magnitude-only modeling framework able to derive stable LTI models for the NTF. It is based on the approximation that the quantization noise is a white and uses output noise spectrum data. For a set of benchmark SDM implementations, we used the proposed approach to verify linearized SDM models used in the literature. Finally, by applying our approach to the class of single-bit MSLA SDMs, we proved that it generalizes to different SDM architectures for which linearized models do not exist. In future work, we intend to apply our modeling framework to multi-bit quantization schemes as well.

Declaration of Competing Interest

The authors declare that they have no known competing financial interests or personal relationships that could have appeared to influence the work reported in this paper.

Acknowledgements

This research is co-financed by Greece and the European Union (European Social Fund-ESF) through the Operational Programme "Human Resources Development, Education and Lifelong Learning" in the context of the project "Strengthening Human Resources Research Potential via Doctorate Research" (MIS-5000432), implemented by the State Scholarships Foundation (IKY).

Appendix A

Eq. (10) can be formulated as the linear system

$$\boldsymbol{Ax} = \boldsymbol{b}. \tag{12}$$

Assuming for now that (at the current iteration) all relocated poles, $a_0, \ldots, a_{N_s-1}$ are real, we define

$$\boldsymbol{A} = \begin{bmatrix} \boldsymbol{\alpha}_0 \\ \vdots \\ \boldsymbol{\alpha}_{N_s-1} \end{bmatrix} \tag{13}$$

where

$$\boldsymbol{\alpha}_k = \left[\frac{1}{z_k - a_1}, \ldots, \frac{1}{z_k - a_n}, 1, \frac{-H(z_k)}{z_k - a_1}, \ldots, \frac{-H(z_k)}{z_k - a_n}\right]$$

for $k = 0, \ldots, N_s - 1$,

$$\boldsymbol{x} = \left[\bar{c}_1, \ldots, \bar{c}_N, \bar{c}_0, \bar{d}_1, \ldots, \bar{d}_N\right]^T$$

and

$$\boldsymbol{b} = [H(z_0), H(z_1), \ldots, H(z_{N_s-1})]^T$$

with $z_k = e^{j\omega_k}$.

The matrices in Eq. (12) contain complex valued entries but $\boldsymbol{x}$ must be real-valued. We consider real-domain arithmetic preferable, therefore for its numerical solution, (12) is transformed into an approximately equivalent form

$$\begin{bmatrix} \mathbb{R}e\{\boldsymbol{A}\} \\ \mathbb{I}m\{\boldsymbol{A}\} \end{bmatrix} \boldsymbol{x} \approx \begin{bmatrix} \mathbb{R}e\{\boldsymbol{b}\} \\ \mathbb{I}m\{\boldsymbol{b}\} \end{bmatrix}. \tag{14}$$

Note that the system $H(z)$ derived by VF must have a real impulse response [39], which is the case if and only if $H(z^*) = H^*(z)$. To achieve this, $\bar{c}_0$ is constrained to take only real values; in addition, if $a_n = a + ja'$ is a pole of the system, then its complex conjugate, $a_{n+1} = a - ja'$ is also a relocated pole of the system and their parameters $\bar{c}_n, \bar{c}_{n+1}$ and $\bar{d}_n, \bar{d}_{n+1}$ should also be complex conjugates pairs, respectively.

Following the above, if one or more relocated poles are complex, we reform system (12). Suppose for example that relocated pole a_1 is complex. Then,

$$\boldsymbol{\alpha}_k = \left[\frac{1}{z_k - a_1}, \frac{1}{z_k - a_1^*}, \ldots\right]$$

and

$$\boldsymbol{x} = \left[\bar{c}_1, \bar{c}_1^*, \ldots,\right]^T$$

are redefined for $k = 0, \ldots, N_s - 1$ as

$$\boldsymbol{\alpha}_k = \left[\left(\frac{1}{z - a_1} + \frac{1}{z - a_1^*}\right), j\left(\frac{1}{z - a_1} - \frac{1}{z - a_1^*}\right), \ldots\right]$$

and

$$\boldsymbol{x} = [\,\mathbb{R}e\{\bar{c}_1\} \quad \mathbb{I}m\{\bar{c}_1\} \quad \ldots],$$

which gives the VF parameters $\bar{c}_1, \bar{c}_2$. Note that the change of representation for d_n, d_{n+1} is similar. By repeating this change of representation for all entries of the system and solving the equivalent system as in (14), we get a real impulse response.

At each iteration, the new set of relocated poles is computed as

$$\boldsymbol{a} = eig\left\{\widehat{\boldsymbol{A}} - \hat{\boldsymbol{b}}\boldsymbol{c}^T\right\} \tag{15}$$

where $\widehat{\boldsymbol{A}} = diag(a_1, a_2, \ldots, a_N)$ contains the relocated poles a_n of the previous iteration, $\hat{\boldsymbol{b}}$ is a column vector of ones and $\boldsymbol{c}^T$ is a row vector containing the residues $\bar{d}_n$.

Again, in the case of complex conjugate relocated poles a_n, a_{n+1}, the entries of the matrices in (15) are constrained to be real by modifying their representation. $\widehat{\boldsymbol{A}}$ becomes a block diagonal matrix with block elements

$$\begin{bmatrix} \mathbb{R}e\{a_1\} & -\mathbb{I}m\{a_1\} & \\ \mathbb{I}m\{a_1\} & \mathbb{R}e\{a_1\} & \\ & & \ddots \end{bmatrix}$$

Similarly, $\hat{\boldsymbol{b}}$ is defined in the block form as

$$\hat{\boldsymbol{b}}_n = [2, 0, \ldots]^T$$

and $\boldsymbol{c}$ with blocks

$$\boldsymbol{c}_n^T = \left[\mathbb{R}e\{\bar{d}_1\}, \ \mathbb{I}m\{\bar{d}_1\}, \ldots\right]$$

respectively.

Appendix B. Supplementary material

Supplementary data associated with this article can be found, in the online version, at https://doi.org/10.1016/j.aeue.2019.152936.

References

[1] Kraus S, Kallfass I, Makon RE, Driad R, Moyal M, Ritter D. A 10-GS/s multibit delta-sigma analog-to-digital converter in an InP HBT technology. In: IEEE Int. Conf. on Microwaves, Communications, Antennas and Electronics Systems (COMCAS). p. 1–4.
[2] Blumgold R, Emami N, Gillen R. Pipelined delta sigma modulator analog to digital converter. In: IEEE Int. Midwest Symp. on Circuits and Systems (MWSCAS). p. 114–8.
[3] Srivastava A, Anantha RR. A programmable oversampling sigma-delta analog-to-digital converter. In: IEEE Int. Midwest Symp. on Circuits and Systems (MWSCAS). p. 539–42.
[4] Kim K, Silva-Martinez J. Low-power 3rd-order continuous-time low-pass sigma-delta analog-to-digital converter for wideband applications. In: IEEE Int. Midwest Symp. on Circuits and Systems (MWSCAS). p. 814–7.
[5] Shu K, Sanchez-Sinencio E, Maloberti F, Eduri U. A comparative study of digital modulators for fractional-N synthesis. In: Proc. IEEE Int. Conf. on Electronics, Circuits and Systems (ICECS); 2001. p. 1391–94.
[6] Tang YL, Ma JG, Xiong F. Implementation of sigma delta modulator for fractional-N frequency synthesis. In: Proc. IEEE international symposium on integrated circuits. p. 497–9.
[7] Su P-E, Pamarti S. Fractional-N phase-locked-loop-based frequency synthesis: A tutorial. IEEE Trans Circ Syst II: Express Briefs 2009;56(12):881–5.

[8] Shin J, Shin H. A 1.9-3.8 GHz ΔΣ fractional-N PLL frequency synthesizer with fast auto-calibration of loop bandwidth and VCO frequency. IE EE J Solid-State Circ 2012;47(3):665–75.
[9] Venkataraman J, Collins O. An all-digital transmitter with a 1-bit. DAC 2007;55(10):1951–62.
[10] Marin R-C, Frappe A, Kaiser A. Digital complex delta-sigma modulators with highly configurable notches for multi-standard coexistence in wireless transmitters, 2017.
[11] Helaoui M, Hatami S, Negra R, Ghannouchi FM. A novel architecture of delta-sigma modulator enabling all-digital multiband multistandard RF transmitters design. IEEE Trans Circ Syst II: Express Briefs 2008;55(11):1129–33.
[12] Kim W-Y, Rode J, Scuderi A, Son H-S, Park CS, Asbeck PM. An efficient voltage-mode class-D power amplifier for digital transmitters with delta-sigma modulation. In: IEEE MTT-S Int. Microwave Symp. Digest (MTT). p. 1–4.
[13] Pan J, Yao L, Lian Y. A sigma-delta class D audio power amplifier in 0.35 μmm CMOS technology. Int. SoC Design Conf. (ISOCC), vol. 1. p. 5–8.
[14] Liu J-M, Chien S-H, Kuo T-H. A 100 W 5.1-channel digital class-D audio amplifier with single-chip design. IEEE J Solid-State Circ 2012;47(6):1344–54.
[15] Janssen E, van Roermund A. Look-ahead based sigma-delta modulation. Springer; 2011.
[16] Christen T. A 15-bit 140-μW scalable-bandwidth inverter-based ΣΔ modulator for a MEMS microphone with digital output. IEEE J Solid-State Circ 2013;48(7):1605–14.
[17] Cardes F, Jevtic R, Hernandez L, Wiesbauer A, Straeussnigg D, Gaggl R. A MEMS microphone interface based on a CMOS LC oscillator and a digital sigma-delta modulator. In: IEEE Int. Symp. on Circ. and Systems (ISCAS). p. 2233–6.
[18] Schreier R, Temes GC. Understanding delta-sigma data converters. John Wiley & Sons Inc; 2005.
[19] Maloberti F. Data converters. 1st ed. Springer; 2007.
[20] Ardalan SH, Paulos JJ. An analysis of nonlinear behavior in Delta-Sigma modulators. IEEE Trans Circ Syst 1987;34(6):593–603.
[21] Sotiriadis PP. Spurs-free single-bit-output all-digital frequency synthesizers with forward and feedback spurs and noise cancellation. IEEE Trans Circ Syst I: Regul Pap 2016;63(5):567–76.
[22] Hosseini K, Kennedy MP. Mathematical analysis of digital MASH delta-sigma modulators for fractional-n frequency synthesis. In: Ph.D Research in microelectronics and electronics. p. 309–12.
[23] Hein S, Zakhor A. On the stability of sigma delta modulators. IEEE Trans Signal Process 1993;41(7):2322–48.
[24] Mladenov V, Hegt H, van Roermund A. Stability analysis of high order sigma-delta modulators. In: Proc. Europ. Conf. on Circuit Theory and Design - ECCTD'01, Espoo, Finland; 2001. p. 313–6.
[25] Vandersteen G, Jain M, Pintelon R. An armax identification method for sigma–delta modulators using only input-output data. IEEE Trans Instrum Meas 2010;59(5):1007–12.
[26] Vandersteen G, Jain M, Pintelon R. Characterization of sigma-delta modulators using armax identification methods. In: 2009 IEEE Instrumentation and measurement technology conference. p. 1485–9.
[27] Schoukens J, Pintelon R, Dobrowiecki T, Rolain Y. Identification of linear systems with nonlinear distortions. Automatica 2005;41(3):491–504. data-Based Modelling and System Identification..
[28] Gustavsen B, Semlyen A. Rational approximation of frequency domain responses by Vector Fitting. IEEE Trans Power Deliv 1999;14(3):1052–61.
[29] de la Rosa JM. Sigma-delta modulators: Tutorial overview, design guide, and state-of-the-art survey. IEEE Trans Circ Syst I: Regul Pap 2011;58(1):1–21.
[30] Hosseini K, Kennedy MP. Maximum sequence length mash digital delta–sigma modulators. IEEE Trans Circuits Syst I: Regul Pap 2007;54(12):2628–38.
[31] Mai D, Kennedy MP. A design method for nested mash-sq hybrid divider controllers for fractional-nfrequency synthesizers. IEEE Trans Circuits Syst I: Regul Pap 2018;65(10):3279–90.
[32] Basetas C, Orfanos T, Sotiriadis PP. A class of 1-bit multi-step look-ahead ΣΔ modulators. IEEE Trans Circuits Syst I: Regul Pap 2017;64(1):24–37.
[33] Bourdopoulos GI, Pnevmatikakis A, Anastassopoulos V, Deliyannis TL. Delta-sigma modulators: modeling, design and applications. Imperial College Press; 2003.
[34] Wang LY, Yin G, Zhang J-F, Zhao Y. System identification with quantized observations. Birkhauser; 2010.
[35] Tommasi LD, Gustavsen B, Dhaene T. Robust transfer function identification via an enhanced magnitude vector fitting algorithm. IET Control Theory Appl 2010;4(7):1169–78.
[36] Hendrickx W, Deschrijver D, Knockaert L, Dhaene T. Magnitude vector fitting to interval data. Math Comput Simul 2009;80(3):572–80.
[37] Oppenheim AV, Schafer RW. Discrete-time signal processing. 2nd ed. Prentice-Hall; 1999.
[38] Mekonnen YS, Schutt-Aine JE. Broadband macromodeling of sampled frequency data using z-domain vector-fitting method. In: 2007 IEEE workshop on signal propagation on interconnects. p. 45–8.
[39] Grivet-Talocia S, Gustavsen B. Passive macromodeling. 1st ed. Wiley; 2016.
[40] Leftreriou S, Antoulas AC. On the convergence of the vector-fitting algorithm. IEEE Trans Microwave Theory Techn 2013;61(4):1435–43.
[41] Wong N, Lei C-U. Iir approximation of fir filters via discrete-time vector fitting. IEEE Trans Signal Process 2008;65(3):1296–302.
[42] Risbo L. Stability predictions for high-order/spl sigma//spl delta/modulators based on quasilinear modeling. In: Proceedings of IEEE International Symposium on Circuits and Systems - ISCAS '94, vol. 5; 1994. p. 361–4.
[43] Schreier R. Delta sigma toolbox (Dec. 2011). http://www.mathworks.com/matlabcentral/fileexchange/19-delta-sigma-toolbox.
[44] Basetas C, Temenos N, Sotiriadis PP. An efficient hardware architecture for the implementation of multi-step look-ahead sigma-delta modulators. In: 2018 IEEE international symposium on circuits and systems (ISCAS). p. 1–5.